The Journal of Laryngology & Otology (2010), ***124***, *48–54.*

doi:10.1017/S0022215109990971

Main Article

Effects of septal perforation on nasal airflow: computer simulation study

H P Lee, R R Garlapati*, V F H Chong†, D Y Wang*

Abstract

Background: Nasal septal perforation is a structural or anatomical defect in the septum. The present study focused on the effects of septal perforation on nasal airflow and nasal patency, investigated using a computer simulation model.

Methods: The effect of nasal septal perforation size on nasal airflow pattern was analysed using computer-generated, three-dimensional nasal models reconstructed using data from magnetic resonance imaging scans of a healthy human subject. Computer-based simulations using computational fluid dynamics were then conducted to determine nasal airflow patterns.

Results: The maximum velocity and wall shear stress were found always to occur in the downstream region of the septal perforation, and could potentially cause bleeding in that region, as previously reported. During the breathing process, there was flow exchange and flow reversal through the septal perforation, from the higher flow rate to the lower flow rate nostril side, especially for moderate and larger sized perforations.

Conclusion: In the breathing process of patients with septal perforations, there is airflow exchange from the higher flow rate to the lower flow rate nostril side, especially for moderate and large sized perforations. For relatively small septal perforations, the amount of cross-flow is negligible. This cross-flow may cause the whistling sound typically experienced by patients.

Key words: Nasal Septum; Perforation; Respiratory Airflow; Computer Simulation

Introduction

Nasal septal perforation is a structural or anatomical defect in the septum. It occurs due to septal submucous resection, and can be caused by septal surgery (e.g. septoplasty), blunt trauma and inhalatory drug abuse, as well as by excessive nose picking, nose packing and cauterisation.[1–3] There are a wide variety of symptoms of nasal septal perforation, including a sensation of nasal obstruction, epistaxis, crusting, dryness, headache, nasal pain and a whistling sound. Septal perforations may typically be classified as asymptomatic, small symptomatic (i.e. smaller than 2 cm in diameter) and large symptomatic (i.e. larger than 2 cm in diameter).[3] Numerous clinical case studies have described the surgical treatments for this condition.[1–6] However, relatively few experimental or computer-based studies have assessed the effects of septal perforation on nasal airflow and patency.

It has been acknowledged that nasal airflow affects the patency and physiological functions of the nose, such as filtration, warming and humidification of inspired air, the sense of smell, and the sensation of nasal pungency.[7]

It is almost impossible to examine and visualise airflow in the nasal cavities *in vivo*. Studies on nasal airflow patterns can only be done using *in vitro* models of the human nose or *in vivo* rodent models. The use of three-dimensional nasal cavity models constructed from magnetic resonance imaging (MRI) and computed tomography (CT) data, coupled with the use of computational fluid mechanics techniques, has been found to be a useful tool and method with which to simulate and understand nasal airflow patterns. Although there are many computational fluid dynamics studies addressing nasal obstruction, turbinate surgery and particle deposition, there are relatively few such studies assessing the effect of nasal septal perforation on nasal airflow.

Among the few reported studies is that of Grant *et al.* who created a three-dimensional nasal cavity model using CT scans from a healthy human subject, and then artificially inserted a virtual septal perforation.[8] It was found that high wall shear stresses were concentrated in the posterior region of the perforation. This finding may explain the typical bleeding associated with septal perforation. However, only a single model was presented.

From the Department of Mechanical Engineering, National University of Singapore, and the Departments of *Otolaryngology and †Diagnostic Radiology, Yong Loo Lin School of Medicine, National University of Singapore.
Accepted for publication: 11 May 2009. First published online 24 September 2009.

Pless *et al.* presented a numerical simulation study of airflow patterns and air temperature distribution during inspiration in a nose model with a septal perforation.[9] They constructed two models with and without septal perforation, based on the CT scan of a healthy human subject. Septal perforation was found to cause highly disturbed airflow in the area of the perforation. The disturbed airflow and temperature distribution across the septal perforation could be a cause of crusting and recurrent nose bleeds.

Grutzenmacher *et al.* were the first to investigate septal perforation related airflow patterns by performing fluid flow experiments on functional nasal models, namely modified Mink boxes.[10] These authors assessed septal perforations of varying sizes and locations, with and without septal deviation. Streamlines were found to 'bump' towards the posterior border of the perforation, causing turbulence which increased with increasing perforation size. In large perforations, it proved impossible to generate a sufficiently high flow velocity to cause a whistling.

In another article, Grutzenmacher and colleagues analysed the effects of septal perforations of varying sizes and locations, using modified Mink boxes representing anatomically exact models of the human nose.[11] The perforation location was found to have no effect on the airflow pattern. In large perforations, the air jet was found to collide with the posterior edge of the perforation and to disintegrate turbulently.

In this study, we investigated the airflow pattern and wall shear stress distribution in a nasal cavity with a septal perforation. We also assessed the effect of septal perforation size. Moreover, we analysed the correlation between the results of engineering simulations (based on computational fluid mechanics) and clinical observations.

Methods

Firstly, representative nasal airway geometry was obtained from the MRI nasal scans of a healthy human subject. Scan slices of 1.5 mm, taken in the coronal plane, were used. These images were segmented and a three-dimensional model was constructed using Mimics version 12.1 software (http://www.materialise.com). An in-house algorithm was used to improve the mesh quality. The resulting three-dimensional nasal cavity model is shown in Figure 1. It can be seen that the model includes all the important features of the nasal cavity. A nasal septal perforation was then created in the model at the location shown in Figure 2. This perforation was cylindrical in shape, with a diameter of 5, 10 or 15 mm for a small, medium or large perforation, respectively. Our 15 mm diameter 'large' perforation was smaller than the 20 mm diameter perforation defined as a large perforation by Heller *et al.*[3] This was because a 20 mm perforation was found to be too large for the relatively smaller Asian nose used in the present model and simulation.

We then constructed high resolution, three-dimensional volume meshes comprising air volume computational domain exterior to the nose (Figure 3) for the various septal perforation sizes used. A typical computational model comprised about 2 million three-dimensional tetrahedral grids. Models were generated using a combination of several commercially available pre-processing software programs, including Mimics version 12.1, Hypermesh version 8.0 (http://www.altair.com) and TGrid version 4.0 (http://truegrid.qarchive.org). Finally, the numerical simulation was carried out using the commercial computational fluid dynamics (CFD) software program Fluent version 6.3.22 (http://www.fluent.com).

For the purposes of this computational fluid dynamics simulation process, the overall flow was assumed to be incompressible, quasi-steady and laminar. At the external boundary of the air volume for the computational domain exterior to the nose, the pressure inlet was applied with zero gauge pressure (i.e. atmospheric pressure). The existence of this extra volume (2040 cm^3) in front of the nose would ensure that the entry of gas was in contact with uniform atmosphere gas and further isolate the artificial boundary condition effect to the simulation results within nasal cavity. A constant nasopharyngeal airflow velocity of 2 m/s (and hence a constant flow rate) was applied as the boundary condition for the simulations. It was assumed that a person suffering from any nasal problems would still desire to inhale the same amount of oxygen (and generate the same flow rate) during the breathing process. However, in order to compare and validate the present model with the reported findings of Grant *et al.*, the velocity boundary condition at the throat was first replaced by a pressure boundary condition of -50 Pa, to match the condition imposed by Grant and colleagues in their modelling and simulation studies.[8]

The project was approved by the institutional review board of the National University of Singapore, as regards its ethical aspects.

Results and discussion

We could make only a qualitative comparison between our findings from the present model and those of Grant *et al.* as these authors did not describe in detail the nasal geometry or the perforation size and location used in their model.[8] Various representative results from our 15 mm perforation model, for the inhalation case study, were compared with Grant and colleagues' results.[8] Firstly, three coronal sections were identified in our model which were similar to those reported by Grant *et al.*[8] (Figure 4). The velocity contours presented in Figure 5 at these three coronal planes, and the velocity contour at and around the perforation, shown in Figure 6, are similar to those presented by Grant *et al.*[8] We also found that high shear stresses concentrated in the posterior region of the perforation (shown in Figure 7), in agreement with Grant and colleagues' findings; this could explain the typical bleeding associated with septal perforation.[8]

https://doi.org/10.1017/S0022215109990971 Published online by Cambridge University Press

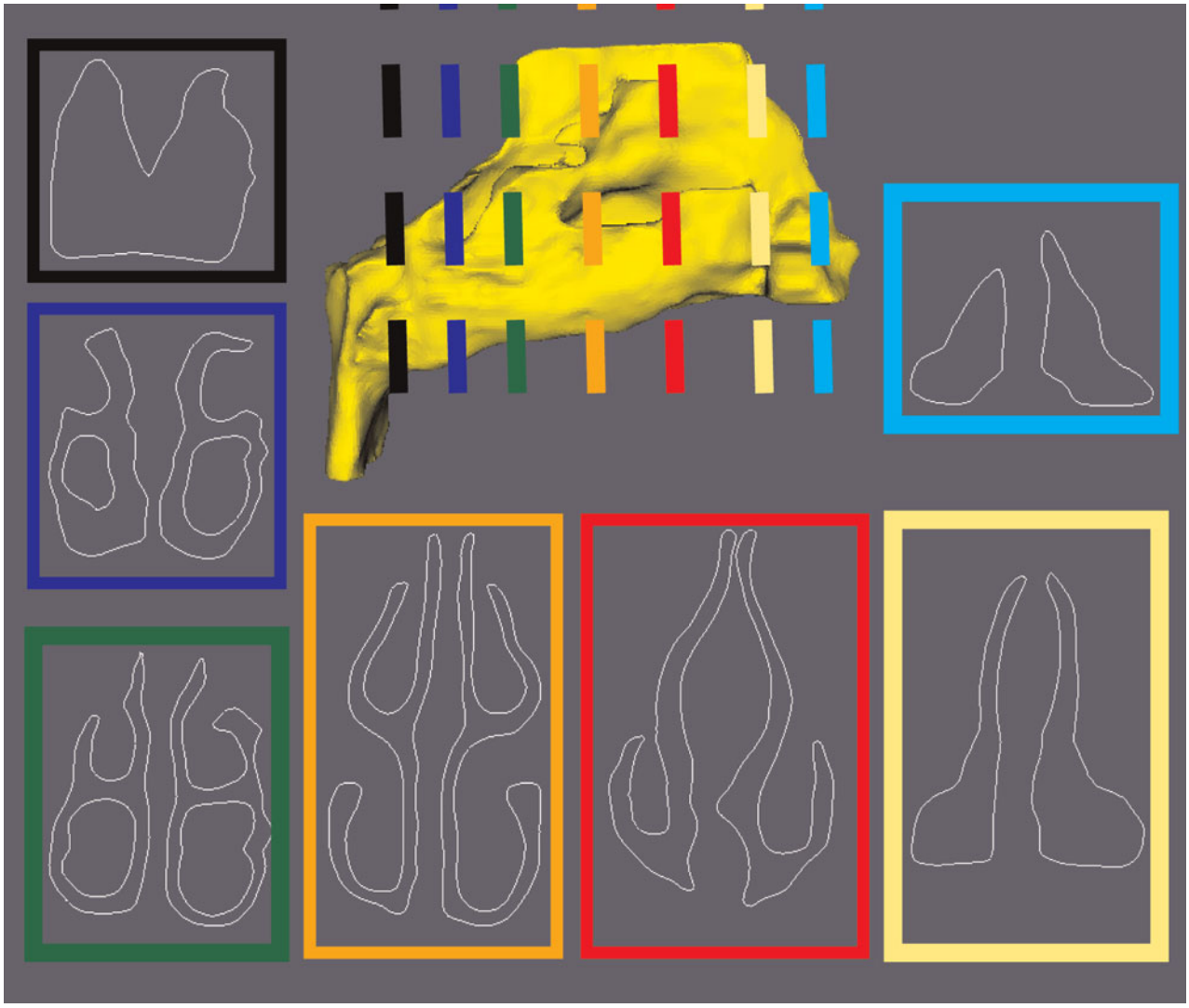

FIG. 1
Sagittal plane view of the three-dimensional nasal cavity model, also showing various cross-sectional, coronal planes indicating the features of the nasal cavity.

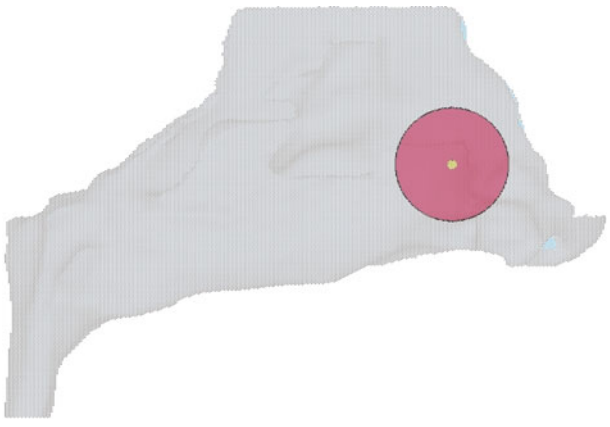

FIG. 2
The location of the septal perforation in the nasal cavity model.

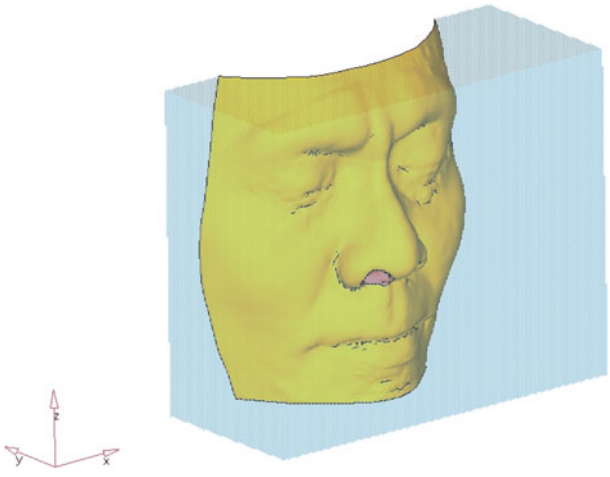

FIG. 3
External computational domain of the nasal cavity.

https://doi.org/10.1017/S0022215109990971 Published online by Cambridge University Press

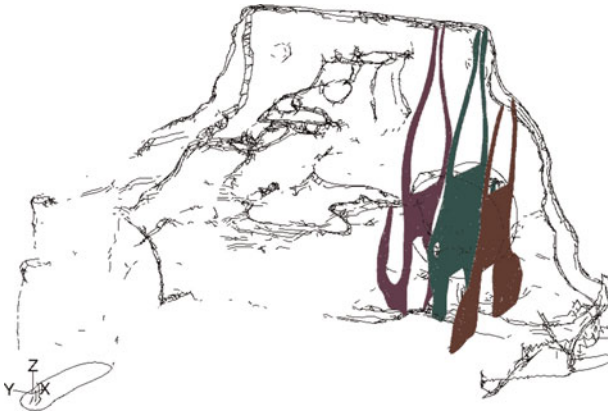

FIG. 4

Location of the three coronal planes. The innermost plane was designated plane (a), followed by plane (b) and plane (c) closest to the nostril.

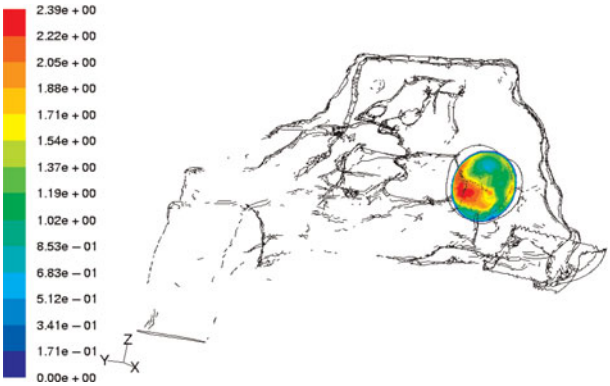

FIG. 6

Velocity contours at and around the septal perforation. Scale indicates colour codes for least (blue) to greatest (red) velocity.

We also used a simulation involving 2 m/s airflow velocity for nasal cavity models with three different sizes of septal perforation. Figures 8 and 9 show velocity contours for the three perforation sizes, for inhalation and exhalation, respectively. Figures 10 and 11 show the wall shear stress contours for the same three perforation sizes, for inhalation and exhalation, respectively.

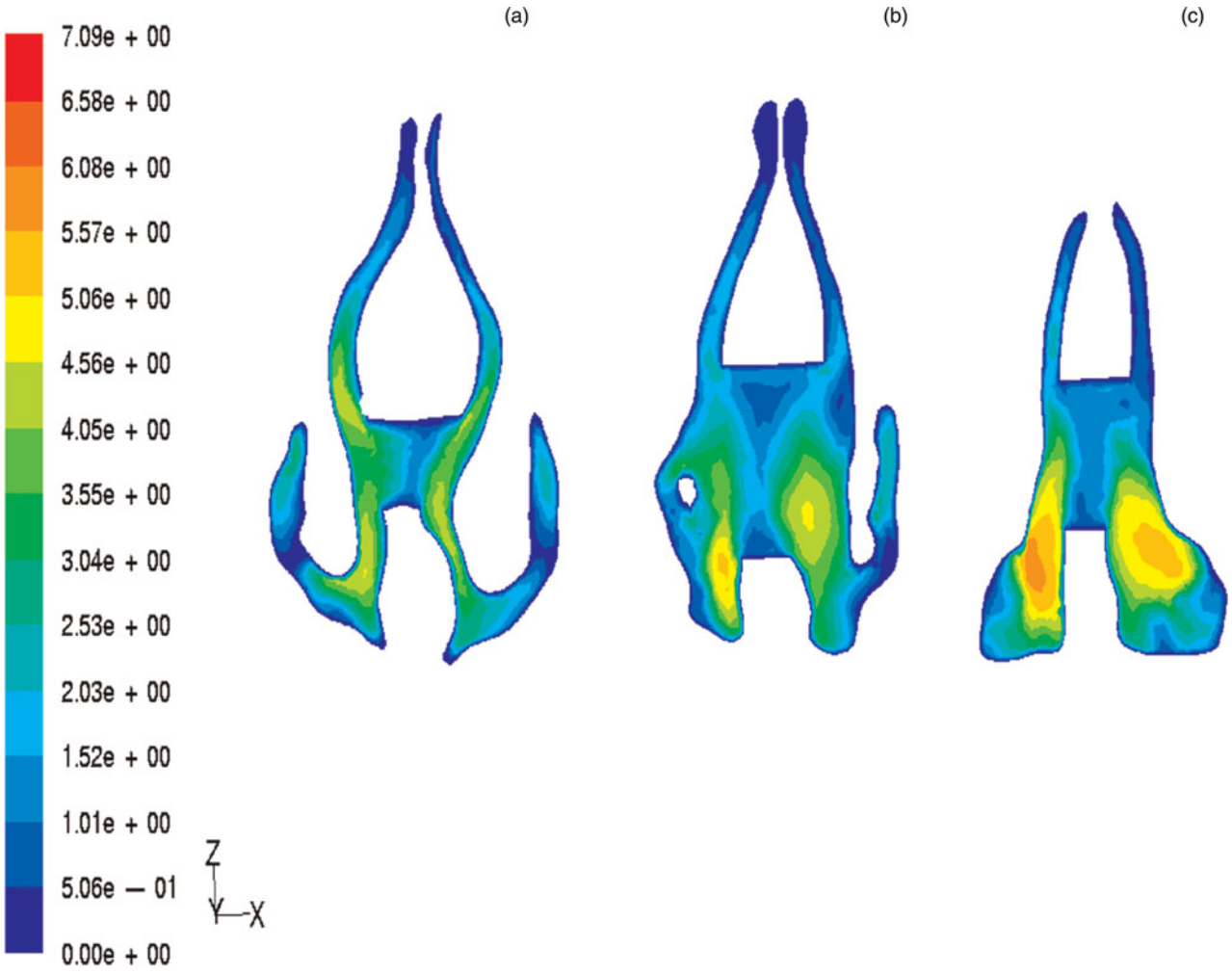

FIG. 5

Velocity contours at the three planes (a), (b) and (c), as defined in Figure 4. Scale indicates colour codes for least (blue) to greatest (red) velocity.

https://doi.org/10.1017/S0022215109990971 Published online by Cambridge University Press

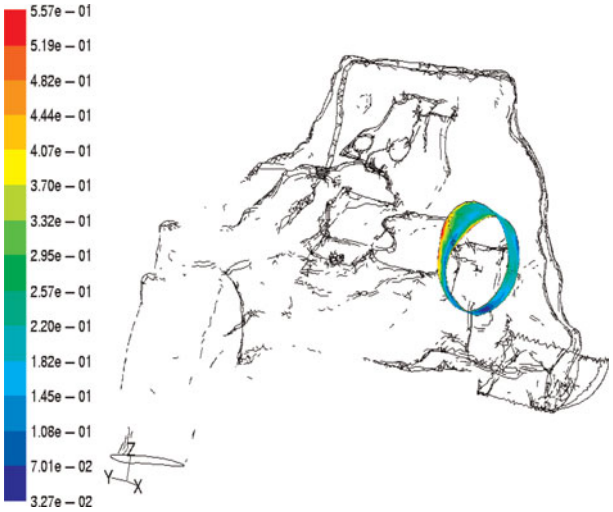

FIG. 7

Wall shear stress contour at and around the perforation. Scale indicates colour codes for least (blue) to greatest (red) shear stress.

It was observed that the maximum velocity and shear stress always occurred in the downstream region of the septal perforation. This could potentially cause bleeding in that particular region, as reported by other researchers.

It was also observed that there was flow exchange through the septal perforation during the breathing process, from the higher flow rate to the lower flow rate nostril side. For the 15 mm septal perforation, this flow exchange was calculated to be 31 cm^3/s in inhalation and 17 cm^3/s in exhalation, thus contributing about 6–10 per cent of the total flow rate (this being 290 cm^3/s). There was a reversal in cross-flow in exhalation compared with inhalation, as shown in Figure 12. The same trends observed for the 15 mm septal perforation were also observed for the 5 and 10 mm perforations.

A key observation was that the cross-flow percentage did not decrease much when the perforation size was reduced from 15 to 10 mm. In contrast, a comparatively large decrease in cross-flow percentage was seen when the perforation size was reduced from 10 to 5 mm. Moreover, it was observed that the septal perforation always resulted in cross-flow from the side with the higher upstream flow rate to the side with the (initial) lower upstream flow rate, for both inhalation and exhalation. For the 10 mm septal perforation, the cross-flow rates were 28 cm^3/s for inhalation and 7 cm^3/s for exhalation. For the 5 mm septal perforation, the cross-flow rates were 13 cm^3/s for inhalation and 7 cm^3/s for exhalation. This cross-flow could be the reason for the whistling sound typically experienced by patients.

In order to verify whether there was a minimal septal perforation size capable of producing cross-flow, the same nasal cavity model was used but with

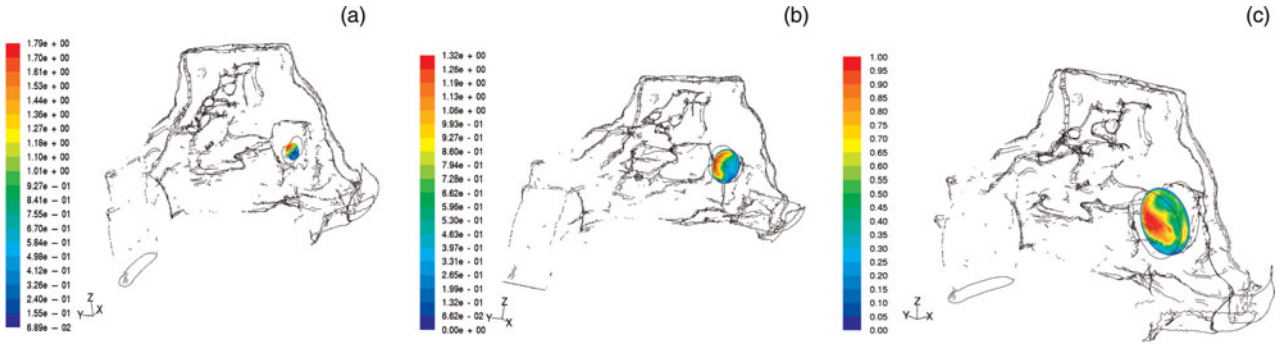

FIG. 8

Velocity contours for inhalation, for (a) 4 mm, (b) 10 mm and (c) 15 mm septal perforations. Scales indicate colour codes for least (blue) to greatest (red) velocity.

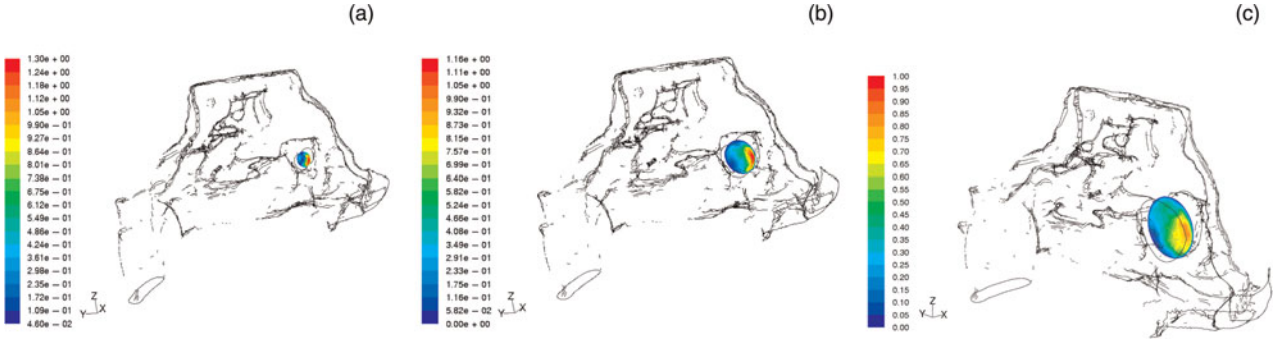

FIG. 9

Velocity profiles for exhalation, for (a) 4 mm, (b) 10 mm and (c) 15 mm septal perforations. Scales indicate colour codes for least (blue) to greatest (red) velocity.

https://doi.org/10.1017/S0022215109990971 Published online by Cambridge University Press

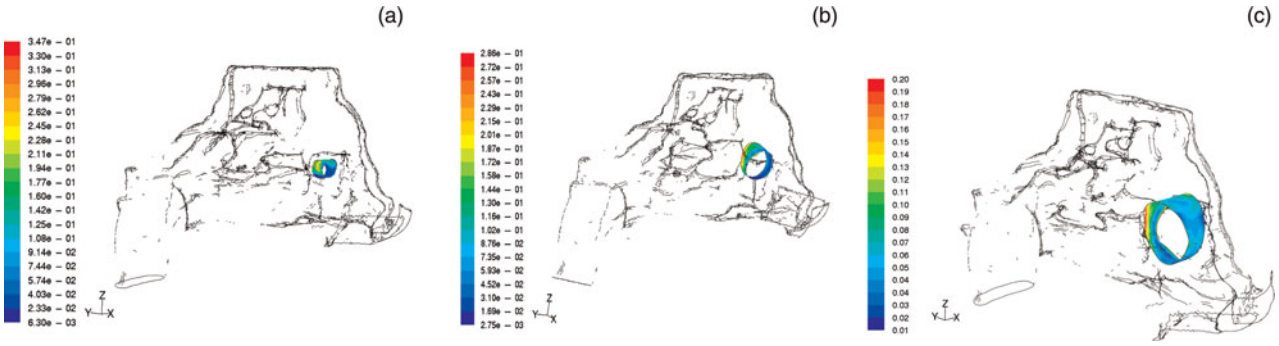

FIG. 10
Wall shear stress profile for inhalation, for (a) 4 mm, (b) 10 mm and (c) 15 mm septal perforations. Scales indicate colour codes for least (blue) to greatest (red) shear stress.

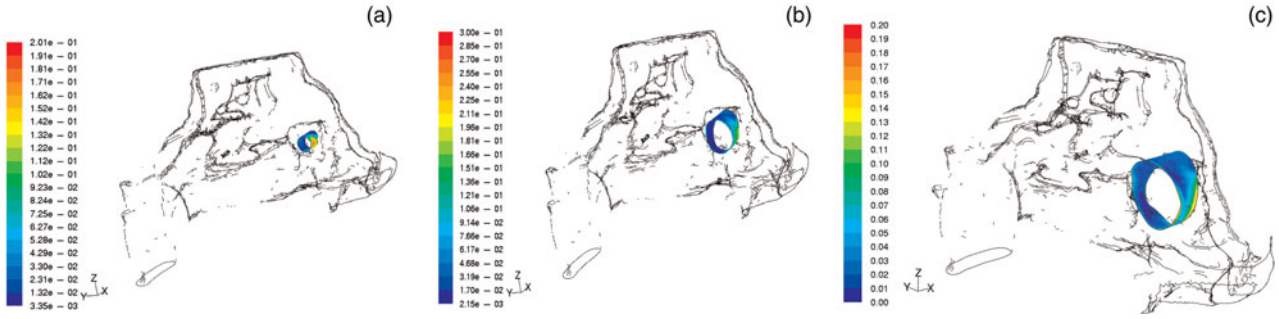

FIG. 11
Wall shear stress profile for exhalation, for (a) 4 mm, (b) 10 mm and (c) 15 mm septal perforations. Scales indicate colour codes for least (blue) to greatest (red) shear stress.

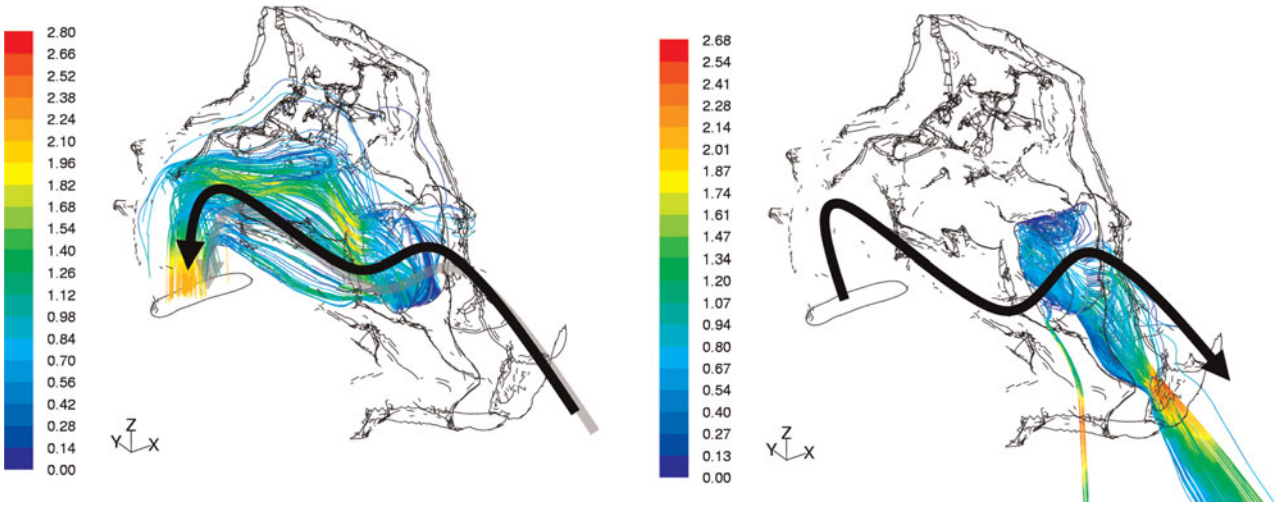

FIG. 12
Reversal in cross-flow direction via the septal perforation during the breathing cycle. Scales indicate colour codes for least (blue) to greatest (red) velocity.

a 1.4 mm diameter perforation at the same location, and the flow pattern evaluated. The amount of cross-flow was negligible (inhalation, 0.3 cm^3/s; exhalation, 0.4 cm^3/s).

The methods of the present study could be extended to investigate the combined effect of septal perforation and septal deviation, as well as the combined effect of septal perforation and nasal obstruction.

The present, numerical study had some limitations, for example the assumption that airflow is incompressible and laminar. One could argue that nasal airflow is not laminar but rather a mixture of turbulent and orifice flow.[12] However, the details

https://doi.org/10.1017/S0022215109990971 Published online by Cambridge University Press

of the respiratory airflow pattern throughout the nasal cavity are not completely understood at present.

- **This study created computer-based nasal models with various sizes of septal perforation, using data from magnetic resonance imaging scans of a healthy human subject**
- **Maximum velocity and shear stress were found always to occur in the downstream region of the septal perforation; this could potentially cause bleeding at this site, as reported by other researchers**
- **During the breathing process, flow exchange through the septal perforation occurred from the higher flow rate to the lower flow rate nostril side**
- **In relatively small septal perforations, the amount of cross-flow was negligible**

The primary aim of the present study was to investigate the effect of septal perforation on normal nasal airflow. Therefore, we did not address other common conditions such as septal deviation. It has been reported that such variables as temperature and humidity can also influence the nasal airflow pattern (altering velocity and turbulence, for instance).[13] In future numerical studies, all these confounding factors would need to be considered in terms of study design and actual experiments.

Conclusion

This study created computer-based nasal models with various sizes of septal perforation, based on MRI scans of a healthy human subject. It was found that the maximum airflow velocity and shear stress always occurred in the downstream region of the septal perforation, and could potentially cause bleeding in that particular region, as reported by other researchers. Flow exchange through the septal perforation was also observed during the breathing process, from the higher flow rate to the lower flow rate nostril side, especially for moderate and large septal perforations. For relatively small septal perforations, the amount of cross-flow was negligible.

Acknowledgements

The authors would like to acknowledge Chiet Sing Chong and Hee Joo Poh, of the Institute of High Performance Computing, for their assistance with image segmentation and model construction. The authors would also like to acknowledge the financial support of an Academic Research Grant from the Ministry of Education, Republic of Singapore.

References

1 Re M, Paqolucci L, Romeo R, Mallardi V. Surgical treatment of nasal septal perforations: our experience. *Acta Otorhinolaryngol Ital* 2006;**26**:102–9
2 Presutti L, Ciufelli MA, Marchioni D, Villari D, Marchetti A, Mattioli A. Nasal septal perforations: our surgical technique. *Otolaryngol Head Neck Surg* 2007;**136**:369–72
3 Heller JB, Gabbay JS, Trussler A, Heller MM, Bradley JP. Repair of large nasal septal perforations using facial artery musculomucosal (FAMM) flap. *Ann Plast Surg* 2005;**55**:456–9
4 Metzinger SE, Guerra AB, Metairie LA. Diagnosing and treating nasal septal perforations. *Aesthet Surg J* 2005;**25**:524–9
5 Mullace M, Gorini E, Sbrocca M, Artesi L, Mevio N. Management of nasal septal perforations using silicone nasal septal button. *Acta Otorhinolaryngol Ital* 2006;**26**:216–18
6 Goh AY, Hussain SSM. Different surgical treatments for nasal septal perforation and their outcomes. *J Laryngol Otol* 2007;**121**:419–26
7 Zhao K, Dalton P. The way the wind blows: implications of modeling nasal airflow. *Curr Allergy Asthma Rep* 2007;**7**:117–25
8 Grant O, Bailie N, Watterson J, Cole J, Gallagher G, Hanna B. Numerical model of a nasal septal perforation. *Medinfo* 2004;**11**:1352–6
9 Pless D, Keck T, Wiesmiller KM, Lamche R, Aschoff AJ, Lindemann J. Numerical simulation of airflow patterns and air temperature distribution during inspiration in a nose model with septal perforation. *Am J Rhinol* 2004;**18**:357–62
10 Grutzenmacher S, Lang C, Saadi R, Mlynski G. First findings about the nasal airflow in noses with septal perforation [in German]. *Laryngorhinootologie* 2002;**81**:276–9
11 Grutzenmacher S, Mlynski R, Lang C, Scholz S, Saadi R, Mlynski G. The nasal airflow in noses with septal perforation: a model study. *ORL J Otorhinolaryngol Relat Spec* 2005;**67**:142–7
12 Eccles R. Nasal airflow in health and disease. *Acta Otolaryngol* 2000;**120**:580–95
13 Lindemann J, Keck T, Wiesmiller K, Sander B, Brambs HJ, Rettinger G *et al.* Nasal air temperature and airflow during respiration in numerical simulation based on multislice computed tomography scan. *Am J Rhinol* 2006;**20**:219–23

Address for correspondence:
Dr Heow Pueh Lee,
Department of Mechanical Engineering,
National University of Singapore,
9 Engineering Drive 1,
Singapore 117576.

Fax: 65 67791459
E-mail: mpeleehp@nus.edu.sg

Dr H P Lee takes responsibility for the integrity of the content of the paper.
Competing interests: None declared